UDK 528.517:528.066:528.11:66.026.2
Original scientific paper / Izvorni znanstveni članak

Modelling the Accuracy Equation of Sokkia 530RK Reflectorless Total Station due to Incident Angle on the Above-Ground Pipeline's Surface

Denys KUKHTAR, Volodymyr ROMANIUK – Ivano-Frankivsk[1], Ihor SAVCHYN – Lviv[2]

ABSTRACT. The specificity of monitoring the above-ground pipelines requires rapid remote measurements. In most cases, it's impossible to set up reflecting prisms on the construction elements to measure distances. Using total stations with reflectorless mode provide fulfilment of these requirements. This article compares the results of a priori and a posteriori accuracy estimation for pipeline coordinate determination by reflectorless total station Sokkia 530RK. This research carried out on the laboratory and field tests, as well as results of surveying on an existing gas pipeline (pipe diameter 1420 mm). The results of experiments showed that the value of horizontal coordinates error exceeds the expected error for incidence angle more than 37°. The values of the vertical position errors of the points exceed the theoretically calculated values for incidence angles more than 33°. The analysis of the error sources on distance determination by the reflectorless mode of total stations was performed. The obtained accuracy equation based on experimental data allows us to determine the distance measurement error according to the distance and incidence angle.

Keywords: reflectorless total station, a priori accuracy estimation, incidence angle, structure monitoring, above-ground pipeline.

1. Introduction

At the present stage of improving geodetic equipment, electronic total stations became widely used with the ability to perform measurements in reflectorless mode. First models of the reflectorless total stations had a number of

[1] Denys Kukhtar, Ph.D., Department of Geodesy and Land Management, Ivano-Frankivsk National Technical University of Oil and Gas, Carpathian 15, UA-76019 Ivano-Frankivsk, Ukraine, e-mail: mailden@meta.ua,
Volodymyr Romaniuk, Ph.D., corresponding author, Department of Geodesy and Land Management, Ivano-Frankivsk National Technical University of Oil and Gas, Carpathian 15, UA-76019 Ivano-Frankivsk, Ukraine, e-mail: volodymyromaniuk@gmail.com,
[2] Ihor Savchyn, Ph.D., Department of Higher Geodesy and Astronomy, Institute of Geodesy, Lviv Polytechnic National University, Karpinskyi str. 6, UA-79013 Lviv, Ukraine, e-mail: savchyn@gmail.com.

limitations. Among them, there were a small range of distance measurement and low accuracy compared with the measurement on the reflecting prism. However, today the main restrictions are eliminated on a constructive level. This made it possible to perform reflectorless measurements for most engineering needs (Ali et al. 2016), volume calculation (Rákay et al. 2013), for remote (Tamagnan and Beth 2012) and automated monitoring (Du et al. 2017). The reflectorless measurements in close range are relevant for indoor and industrial applications (Zámećníková et al. 2014) as well as long-range measurements (Khalil 2015).

Most of the projects require observing points that are not available to install a reflector on them, or are situated in a dangerous place for people to stay in the area. In such cases, preference is given to reflectorless total stations. They make it possible not only to conduct measurements remotely but also to reduce the time of surveying.

The studies presented in this article were carried out with the aim of improving the methodology for monitoring the above-ground gas pipelines which cross natural and artificial obstacles (Fig. 1).

According to the results of previous studies carried out by the authors (Trevoho et al. 2011), the location of setting up total stations has been substantiated to allow maximum productivity during the observation. The position of the instrument at

Fig. 1. *An above-ground gas pipeline with diameter 1420 mm. The Carpathians, Ukraine (UKRTRANSGAZ 2015).*

a distance of 45 m from the axis of the pipeline is optimal. In this case, the maximum horizontal incidence angle is 54°.

An unsolved problem is the preliminary estimation of the coordinate accuracy of pipeline axis which measured by a total station in reflectorless mode.

The technique of researching the reflectorless mode of a total station, which is chosen by most scientists, involves determining the accuracy of the distance measurement for different incidence angles to the reflecting surfaces. The results of experimental studies, performed for various models of total stations, confirm the increasing of error measurements with increasing of incidence angle (Gairns 2008, Fawzy 2015). The magnitude of the maximum incidence angle depends on the color and structure of the material that should be monitored. This is evidenced by the results of Mazalová et al. (2009) studies, Lambrou and Pantazis (2010), Daliga and Kuraĺowicz (2016), Lambrou (2018).

For the preliminary estimation of the accuracy of linear measurements, manufacturers of total stations offer the using of the known formula (Jeźko 2014, Barković et al. 2016):

$$m_S = a + b \cdot 10^{-6}\,, \tag{1}$$

where a represents the additive element and b is the scale element. In this formula, the value of b is variable and depends on the length of the line being measured.

The results of numerous experiments (Gairns 2008, Mazalová et al. 2009, Lambrou and Pantazis 2010, Fawzy 2015, Jeźko 2014) show that the error of measurement of distance correlates with the magnitude of the incidence angle to the surface. Therefore, we suppose that Eq. 1 can be improved. To do this, we need to enter an additional factor that takes into account the incidence angle when performing reflectorless measurements. Thus, the accuracy of the distance measurement can be expressed by the function of the distance S and the beam's incidence angle β:

$$m_S = f\left(\beta; S\right). \tag{2}$$

2. Materials and Methods

A reflectorless total station Sokkia 530RK was used to observe the deformations of the above-ground gas pipelines. The accuracy of this instrument was sufficient for monitoring (Kukhtar 2017).

In order to obtain data on the accuracy of the measurements, we performed experimental studies of the Sokkia 530RK total station in the reflectorless mode when observing the surface of the above-ground pipeline.

2.1. Field surveying test

Observations were made according to the scheme presented in Fig. 2. The total station is set at point A at a distance of 45 m from the axis of the pipeline. Seven

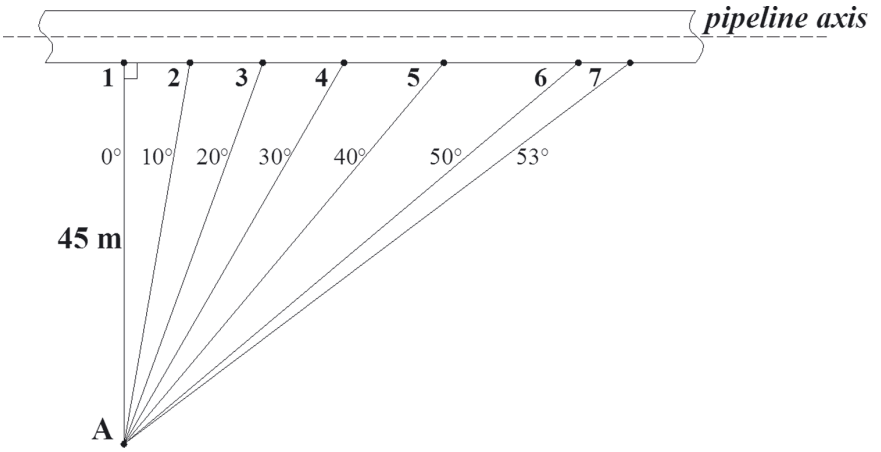

Fig. 2. *Scheme of accuracy determining of points coordinates on pipeline (Trevoho et al. 2011).*

points are marked on the pipeline surface. The horizontal incidence angle for each subsequent point increased from 0° (point 1) to a maximum value of 53° (point 7) in increments of 10° (Fig. 2). The coordinates of seven points were determined 30 times. Observations were carried out in the reflectorless mode of the total station.

2.2. Accuracy estimation of the reflectorless measurements results

A priori accuracy estimation

The accuracy of determining the coordinates of the points varies depending on the measured distance and angle. Therefore, coefficients of the weight matrix for different points are different. The coordinates of the points on the pipeline surface are obtained indirectly by angular and linear measurements. They are calculated according to the well-known formulas of the 3D-polar method:

$$\begin{aligned} X_i &= X_0 + \Delta x = X_0 + S\cos\nu\cos\beta \\ Y_i &= Y_0 + \Delta y = Y_0 + S\cos\nu\sin\beta \\ H_i &= H_0 + \Delta h = H_0 + S\sin\nu \end{aligned} \tag{3}$$

where X_0, Y_0, H_0 are coordinates of the starting point on which the total station is set up; Δx, Δy, Δh – increase of coordinates; S – measured slope distance; β – measured horizontal angle; ν – measured vertical angle.

As the directly observed values are horizontal and vertical angles and distances, the covariance rule is used to obtain the mean square errors of the point coordinates. In accordance with this rule, the matrix $\mathbf{C_P}$ of mean square errors of the point coordinates determines by the formula (Shults and Roshchyn 2016):

$$\mathbf{C_P} = \mathbf{A}\cdot\mathbf{C_L}\cdot\mathbf{A^T} = \begin{pmatrix} m_X^2 & c_{XY} & c_{XH} \\ c_{XY} & m_Y^2 & c_{YH} \\ c_{XH} & c_{YH} & m_H^2 \end{pmatrix}, \tag{4}$$

where $\mathbf{C_L}$ – covariance matrix; $\mathbf{A}$ – a matrix of partial derivatives; m_X, m_Y, m_H – Root Mean Square (RMS) errors of the corresponding coordinates; c_{ij} – correlation moments. The matrix $\mathbf{C_L}$ without correlation relations has the form:

$$\mathbf{C_L} = \begin{pmatrix} m_S^2 & 0 & 0 \\ 0 & m_\nu^2 & 0 \\ 0 & 0 & m_\beta^2 \end{pmatrix}, \tag{5}$$

where m_S, m_ν, m_β – RMS error of distance measurement, vertical angle measurement, and horizontal angle measurement. These values were taken from total station passport.

By differentiating Eq. 3 we find the coefficients of the matrix $\mathbf{A}$ of partial derivatives:

$$\mathbf{A} = \begin{pmatrix} \frac{\partial \Delta x}{\partial S} & \frac{\partial \Delta x}{\partial \nu} & \frac{\partial \Delta x}{\partial \beta} \\ \frac{\partial \Delta y}{\partial S} & \frac{\partial \Delta y}{\partial \nu} & \frac{\partial \Delta y}{\partial \beta} \\ \frac{\partial \Delta h}{\partial S} & \frac{\partial \Delta h}{\partial \nu} & \frac{\partial \Delta h}{\partial \beta} \end{pmatrix} = \begin{pmatrix} \cos\beta\cos\nu & -S\cos\beta\sin\nu & -S\sin\beta\cos\nu \\ \sin\beta\cos\nu & -S\sin\beta\sin\nu & S\cos\beta\cos\nu \\ \sin\nu & S\cos\nu & 0 \end{pmatrix}. \tag{6}$$

Using the Eq. 3 – Eq. 6, and considering that the Sokkia 530 RK total station (m_S = 3 mm, $m_{\nu,\beta}$ = 5'') was used for measurements, we perform a priori estimation of the coordinates accuracy for points 1–7 on the pipeline (Fig. 2). The results of calculations are presented in Table 1.

A posteriori accuracy estimation

For the accuracy estimation was made 30 measurements of the coordinates for each of seven points on the pipeline. As a result, 30 values of distance, 30 values of vertical and horizontal angles were obtained. Therefore, we have a total number of unknowns t=3 and a number of measurements n=90. Consequently, the system of equations, which reflects the process of measurements, is redefined. This allows as to find an adjusted coordinates value, as well as to evaluate the accuracy of the obtained results. We apply the parametric method of alignment to do this (Okwuashi and Asuquo 2014).

The relationship between observed values and adjusted coordinates are presented by the following relations:

$$\begin{aligned} f_1 &= \sqrt{x_i^2 + y_i^2 + h_i^2} = S_i + v_i \\ f_2 &= ar\,\mathrm{ctg}\,\frac{h_i}{\sqrt{x_i^2 + y_i^2}} = \nu_i + v_i\,, \\ f_3 &= ar\,\mathrm{ctg}\,\frac{y_i}{x_i} = \beta_i + v_i \end{aligned} \tag{7}$$

where v_i – residuals for measured values.

The system of residuals equations in a general form can be written as:

$$\begin{aligned}
&\frac{\partial f_1}{\partial x}\delta x + \frac{\partial f_1}{\partial y}\delta y + \frac{\partial f_1}{\partial h}\delta h + (S_0 - S_i) = v_{Si} \\
&\frac{\partial f_2}{\partial x}\delta x + \frac{\partial f_2}{\partial y}\delta y + \frac{\partial f_2}{\partial h}\delta h + (\nu_0 - \nu_i) = v_{\nu i} \\
&\frac{\partial f_3}{\partial x}\delta x + \frac{\partial f_3}{\partial y}\delta y + \frac{\partial f_3}{\partial h}\delta h + (\beta_0 - \beta_i) = v_{\beta i}
\end{aligned} . \tag{8}$$

Let's make changes:

$$\left(\frac{\partial f_i}{\partial x}\right) = a_i \;;\; \left(\frac{\partial f_i}{\partial y}\right) = b_i \;;\; \left(\frac{\partial f_i}{\partial h}\right) = c_i \;;$$

$$S_0 - S_i = l_{Si} \;;\; \nu_0 - \nu_i = l_{\nu i} \;;\; \beta_0 - \beta_i = l_{\beta i} \,. \tag{9}$$

Then linear equations system (Eq. 8) may be written in a matrix form:

$$\begin{pmatrix} a_1 & b_1 & c_1 \\ a_2 & b_2 & c_2 \\ \dots & \dots & \dots \\ a_n & b_n & c_n \end{pmatrix} \cdot \begin{pmatrix} \delta x \\ \delta y \\ \dots \\ \delta z \end{pmatrix} + \begin{pmatrix} l_1 \\ l_2 \\ \dots \\ l_n \end{pmatrix} = \begin{pmatrix} v_1 \\ v_2 \\ \dots \\ v_n \end{pmatrix}, \tag{10}$$

or in a shorter form:

$$\mathbf{A} \cdot \boldsymbol{\delta} + \mathbf{L} = \mathbf{V} \,. \tag{11}$$

The coefficients of the matrix **A**, which has size (90×3), are obtained by differentiating the functions (Eq. 7). Then Eq. 10 has such a form:

$$\begin{pmatrix} \cos\nu_i \cos\beta_i & \cos\nu_i \sin\beta_i & \sin\nu_i \\ \dots & \dots & \dots \\ -\dfrac{\cos\beta_i \sin\nu_i}{S_i} & -\dfrac{\sin\beta_i \sin\nu_i}{S_i} & -\dfrac{\cos\nu_i}{S_i} \\ \dots & \dots & \dots \\ -\dfrac{\sin\beta_i}{S_i \cos\nu_i} & -\dfrac{\cos\beta_i}{S_i \cos\nu_i} & 0 \end{pmatrix} \cdot \begin{pmatrix} \delta x \\ \delta y \\ \delta h \end{pmatrix} + \begin{pmatrix} l_1 \\ l_2 \\ l_3 \\ \dots \\ l_{90} \end{pmatrix} = \begin{pmatrix} v_1 \\ v_2 \\ v_3 \\ \dots \\ v_{90} \end{pmatrix}. \tag{12}$$

Since the coordinates, as well as their increments (vector **δ**), are not directly measured values, we introduce a weight matrix of measurements for the correct calculation of the residual values v_i. The weight matrix $\mathbf{P_i}$ with size (90×90) has a diagonal form:

$$\mathbf{P_i} = \begin{pmatrix} \frac{1}{m_{Si}^2} & 0 & 0 & 0 & 0 & 0 & 0 & 0 & 0 \\ 0 & ... & 0 & 0 & 0 & 0 & 0 & 0 & 0 \\ 0 & 0 & \frac{1}{m_{S30}^2} & 0 & 0 & 0 & 0 & 0 & 0 \\ 0 & 0 & 0 & \frac{1}{m_{vi}^2} & 0 & 0 & 0 & 0 & 0 \\ 0 & 0 & 0 & 0 & ... & 0 & 0 & 0 & 0 \\ 0 & 0 & 0 & 0 & 0 & \frac{1}{m_{v30}^2} & 0 & 0 & 0 \\ 0 & 0 & 0 & 0 & 0 & 0 & \frac{1}{m_{\beta i}^2} & 0 & 0 \\ 0 & 0 & 0 & 0 & 0 & 0 & 0 & ... & 0 \\ 0 & 0 & 0 & 0 & 0 & 0 & 0 & 0 & \frac{1}{m_{\beta 30}^2} \end{pmatrix}. \quad (13)$$

The system of normal equations has a well-known form (Okwuashi and Asuquo 2014):

$$\mathbf{N\delta} + \mathbf{L} = 0\,, \quad (14)$$

where $\mathbf{N} = \mathbf{A^T PA}$ – a square matrix of coefficients of normal equations; $\mathbf{L} = \mathbf{A^T Pl}$ – the vector of free members of normal equations. The vector $\boldsymbol{\delta}$ can be found according to the following scheme:

$$\boldsymbol{\delta} = -\mathbf{N}^{-1} \cdot \mathbf{L}\,. \quad (15)$$

The solution of the normal equations system is coordinate increments. After finding the comparable coordinates, we determine the residuals v_i. The RMS error of the weight μ is found by the formula (Fan 2010):

$$\mu = \sqrt{\frac{\mathbf{V^T PV}}{n-k}}\,, \quad (16)$$

where n=90 number of measurements, k=3 the number of required measurements.

RMS errors of abscissa m_x, ordinate m_y and applicate m_h i-th point found out from the matrix, which obtained by multiplying the square error of the weight μ on the matrix $\mathbf{C_P}$ (Eq. 4):

$$\mathbf{M^2} = \mu^2 \mathbf{C_P} = \mu^2 \begin{pmatrix} C_{xx} & C_{xy} & C_{xh} \\ C_{yx} & C_{yy} & C_{yh} \\ C_{hx} & C_{hy} & C_{hh} \end{pmatrix}, \quad (17)$$

then

$$m_X = \mu\sqrt{C_{xx}}\ ,\ \ m_Y = \mu\sqrt{C_{yy}}\ ,\ \ m_h = \mu\sqrt{C_{hh}}\ . \tag{18}$$

The RMS error of the horizontal position of the point on the pipeline is calculated by the formula:

$$m_{xy} = \sqrt{m_{X_i}^2 + m_{Y_i}^2}\ . \tag{19}$$

The results of computing the RMS error of coordinates by the total station in the reflectorless mode at a distance of 45 meters from the pipeline are presented in Table 1. For comparing, Table 1 also shows the results of a priori accuracy estimation for the respective distances and incidence angles.

Table 1. *Root mean square errors of horizontal and vertical position of control points.*

Number of points	Incidence angle, β [degree]	RMS error of horizontal position		RMS error of vertical position	
		A priori estimation $m_{xy}^{pr.}$ [mm]	A posteriori estimation m_{xy} [mm]	A priori estimation $m_h^{pr.}$ [mm]	A posteriori estimation m_h [mm]
1	0°	3.2	2.0	1.1	0.7
2	10°	3.2	2.0	1.1	0.7
3	20°	3.2	2.3	1.2	0.8
4	30°	3.3	2.8	1.3	1.1
5	40°	3.3	3.6	1.4	1.8
6	50°	3.4	4.8	1.7	2.5
7	53°	3.5	5.8	1.8	2.5

The graphs in Fig. 3 are presented data from Table 1.

Fig. 3 illustrates that the horizontal coordinates accuracy does not exceed theoretically calculated value for incidence angle less than 37°. While incidence angle increase from 37° to the limiting angle of 53°, the coordinates accuracy varies from 3.3 mm to 5.8 mm. The obtained values of the vertical position errors of the points exceed the theoretically calculated values for incidence angles more than 33°.

Error ellipse computation

It is known that the error m_{xy} is used based on the assumption that the error distribution of measurements along X and Y axes has the same probability. The orientation and dimensions of error ellipse semi axis determine the most probable

Fig. 3. *RMS errors of (a) horizontal and (b) vertical position of control points on a pipeline by the estimated and measured values.*

directions and magnitude of maximum and minimum coordinates errors. The Eq. 17 is used to find the elements of the error ellipse for the horizontal errors (Fan 2010). It is known that by rotation of coordinate axes at a certain angle φ, a system UV with the non-diagonal elements of the matrix $\mathbf{C_P}$ equal zero, can be chosen. Then Eq. 17 has such form:

$$\mathbf{M^2} = \mu^2 \begin{pmatrix} C_{UU} & 0 \\ 0 & C_{VV} \end{pmatrix}. \tag{20}$$

The rotation angle φ, which is necessary for such conversion, can be calculated by the formula:

$$\operatorname{tg} 2\varphi = \frac{2C_{xy}}{C_{xx} - C_{yy}}, \tag{21}$$

where the elements C_{UU}, C_{VV} are obtained from equations:

$$\begin{aligned} C_{UU} &= \frac{1}{2}\left\{C_{xx} + C_{yy} + \sqrt{(C_{xx} - C_{yy})^2 + 4C_{xy}^2}\right\} \\ C_{VV} &= \frac{1}{2}\left\{C_{xx} + C_{yy} - \sqrt{(C_{xx} - C_{yy})^2 + 4C_{xy}^2}\right\} \end{aligned}. \tag{22}$$

The values of semi-major and semi-minor axis of the error ellipse were obtained by following formulas:

$$a = \mu\sqrt{C_{UU}}\ ,\ b = \mu\sqrt{C_{VV}}\ . \tag{23}$$

The elements of error ellipses, which were calculated by the algorithm Eq. 21 – Eq. 23, are presented in Fig. 4.

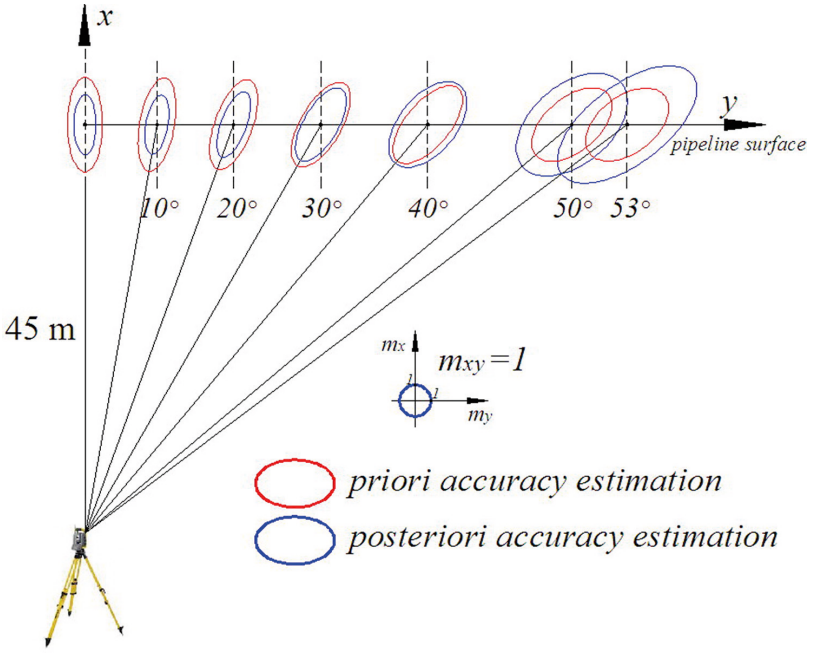

Fig. 4. *Error ellipses of control points on the pipeline surface.*

As we can see in Fig. 4, the value of a posteriori accuracy estimation exceeds the value of a priori accuracy estimation for incidence angles more than 30°. These data coincide with the corresponding values presented in Fig. 3.

Therefore, we can't carry out a preliminary estimation of the coordinates accuracy for incidence angles more than 30°. This is due to an increasing of the linear measurements error.

To solve this problem, the Eq. 1 requires to takes into account the incidence angle to the measured surface. The construction of this model requires the collection of empirical data, which will show the relationship between distance, incidence angle and the accuracy of linear measurement in the reflectorless mode.

2.3. The study of distance measurement accuracy in the reflectorless mode

In order to study the coordinates accuracy using a reflectorless total station for different distances and for different incidence angles, the following experiment was conducted.

A flat target with size 300×300 mm was made to simulate the pipeline surface. The target surface was covered with silver paint which used as anticorrosive coating for above-ground pipeline. It was attached on the telescope of the theodolite. This allowed to rotate the target in a horizontal plane at a defined angle.

The experiment was conducted according to the following scheme. The theodolite with the target was set at the one end of 100-meters length line. The distance from the total station to the target has been changed in a range from 10 m to 100 m with 5m increments. The horizontal incidence angle has been changed from 0° to the maximum value with 10° increments. At each installation, 30 measurements of distance were performed.

The RMS errors of distance measurement were calculated using the Bessel's formula:

$$m_S = \sqrt{\frac{[\Delta\Delta]}{n-1}}, \tag{24}$$

where Δ – deviation from the average value, $n=30$ – number of measurements.

The results of the experiment are presented in Table 2. For comparison, the table also presents the results of a priori accuracy estimation of distance measurements (in brackets).

A table representation of the research results makes it easy to analyze the obtained data. In Table 2 blue cells are cells where values of distance measurements accuracy do not exceed preliminary estimation.

The described above experiment was conducted at the temperature range from +3 °C to +14 °C and cloudy weather. This made it possible to reduce the effect of refraction and high illumination which reduces the accuracy of laser devices.

Table 2. *Root mean square errors of distance measurement, m_S [mm].*

Distance S_i [m]	Rotation angle β_i [degree]								
	0°	10°	20°	30°	40°	50°	60°	70°	80°
10	0.6 (3.0)	0.9 (3.0)	0.9 (3.0)	1.3 (3.0)	1.6 (3.0)	2.0 (3.0)	2.0 (3.0)	2.6 (3.0)	3.2 (3.0)
15	0.9 (3.0)	1.1 (3.0)	1.2 (3.0)	1.3 (3.0)	1.7 (3.0)	1.4 (3.0)	2.2 (3.0)	2.6 (3.0)	3.5 (3.0)
20	0.8 (3.0)	1.1 (3.0)	1.0 (3.0)	1.0 (3.0)	1.6 (3.0)	1.9 (3.0)	2.4 (3.0)	3.1 (3.0)	4.3 (3.0)
25	1.0 (3.1)	1.0 (3.1)	1.0 (3.1)	1.1 (3.1)	1.8 (3.1)	2.4 (3.1)	2.9 (3.1)	4.5 (3.1)	5.2 (3.1)
30	0.8 (3.1)	1.7 (3.1)	1.6 (3.1)	1.6 (3.1)	1.8 (3.1)	2.4 (3.1)	3.4 (3.1)	4.8 (3.1)	–
35	0.7 (3.1)	1.6 (3.1)	1.9 (3.1)	2.1 (3.1)	2.4 (3.1)	2.8 (3.1)	3.8 (3.1)	4.7 (3.1)	–
40	0.9 (3.1)	1.5 (3.1)	2.9 (3.1)	2.8 (3.1)	3.0 (3.1)	3.2 (3.1)	4.0 (3.1)	4.8 (3.1)	–
45	0.7 (3.1)	1.1 (3.1)	1.5 (3.1)	2.5 (3.1)	2.6 (3.1)	3.2 (3.1)	3.5 (3.1)	–	–
50	0.9 (3.1)	1.2 (3.1)	1.4 (3.1)	2.0 (3.1)	2.6 (3.1)	3.3 (3.1)	5.1 (3.1)	–	–
55	1.3 (3.1)	2.0 (3.1)	2.1 (3.1)	2.4 (3.1)	3.2 (3.1)	3.5 (3.1)	5.7 (3.1)	–	–
60	1.3 (3.1)	2.1 (3.1)	2.6 (3.1)	3.3 (3.1)	4.4 (3.1)	4.1 (3.1)	–	–	–
65	1.4 (3.1)	1.8 (3.1)	2.8 (3.1)	3.1 (3.1)	4.3 (3.1)	4.8 (3.1)	–	–	–
70	1.6 (3.1)	2.0 (3.1)	2.7 (3.1)	4.2 (3.1)	4.2 (3.1)	–	–	–	–
75	1.4 (3.2)	1.4 (3.2)	3.3 (3.2)	4.9 (3.2)	–	–	–	–	–
80	1.1 (3.2)	2.3 (3.2)	3.3 (3.2)	4.8 (3.2)	–	–	–	–	–
85	1.4 (3.2)	2.3 (3.2)	3.6 (3.2)	5.2 (3.2)	–	–	–	–	–
90	1.7 (3.2)	3.1 (3.2)	4.1 (3.2)	5.3 (3.2)	–	–	–	–	–
100	1.8 (3.2)	3.2 (3.2)	5.2 (3.2)	5.6 (3.2)	–	–	–	–	–

2.4. Analytical representation of empirical data

In order to describe the measurement results with the analytical model, the influence of error sources should be considered on distance determining in the reflectorless mode of a total station. In expanded form, Eq. 1 could be written (Lobachev 1980):

$$m_S = \sqrt{\left(\frac{v}{pf}\right)^2 m_\varphi^2 + m_d^2 + m_l^2 + S^2\left[\left(\frac{m_f}{f}\right)^2 + \left(\frac{m_v}{v}\right)^2\right]}, \tag{25}$$

where m_φ – RMS error of phase registration, m_d – RMS error of the phase of voltage reference, m_l – RMS error of the instrument constant, m_f – RMS error of the scale frequency, m_v – RMS error of the electromagnetic waves velocity.

The sum of RMS errors that do not depend on the measured length was marked through:

$$P = \left(\frac{v}{pf}\right)^2 m_\varphi^2 + m_d^2 + m_l^2 , \tag{26}$$

and the sum of square relative errors that are proportional to the measured length, through:

$$Q = \left(\frac{m_f}{f}\right)^2 + \left(\frac{m_v}{v}\right)^2 . \tag{27}$$

The Eq. 25 can be noted in such form:

$$m_S = \sqrt{P + Q \cdot S^2} . \tag{28}$$

However, widespread Eq. 1 is used more often which is the linear approximation of the curve corresponding to the Eq. 28. The linear regression equation of reflectorless total station Sokkia 530RK, which was used for measurements, has the form $m_S = \pm(3 + 2 \cdot S \cdot 10^{-6})$.

The experiment results (Table 2) show that the value of RMS error m_S exceeds a priori value for a large incident angle. In order to present the obtained empirical data in a mathematical form, we use the algorithm shown below.

The distance measurements accuracy was determined at different distances for nine positions of incident angle (range 0°–80° with 10° increments). Therefore we wrote nine linear regression equations, based on the data in Table 2. The values of the parameters a and b are determined by the least square method, using measured data. For this purpose, the residual equations are made:

$$a + b \cdot S_i + l_i = v_i , \tag{29}$$

where $l_i = -|m_S|$. The system is overdetermined (the number of equations – 18; the number of unknowns – 2) The system of equations (Eq. 29) has been solved by the least square method with taking into account the diagonal matrix of weight **P**:

$$\mathbf{P} = \begin{pmatrix} \frac{100}{D_1} & 0 & 0 & 0 \\ 0 & \frac{100}{D_2} & 0 & 0 \\ 0 & 0 & \ldots & 0 \\ 0 & 0 & 0 & \frac{100}{D_n} \end{pmatrix} . \tag{30}$$

The calculation results of the coefficients a and b are given in Table 3.

Table 3. *Coefficients of linear regression equation.*

Incidence angle, β [degree]	***a*** **[mm]**	$\boldsymbol{b \cdot S \cdot 10^{-5}}$ **[mm]**
0°	0.6	1
10°	0.7	2
20°	0.5	4
30°	0.4	5
40°	0.9	4
50°	1.2	5
60°	1.6	6
70°	1.7	9
80°	1.8	13

Looking at the obtained data, we see that the coefficient a (errors that do not depend on measured length) and the coefficient b (errors that are proportional to measured length) increase with the changing of incidence angle. Let's analyze the nature of these dependencies based on the data known to us (Schäfer 2017). The RMS error of the phase of voltage reference m_d and the error of the instrument constant m_l are components of a coefficient. They do not depend on the length of measured distance and will not change when the incidence angle β increases. The third component of the coefficient a is the error of phase registration m_φ. It's value depends on the level of reflecting signal, which is taken back from the measured distance. It is known that the error of phase registration does not depend on measured length for distance values that are substantially less than the maximum range. The intensity of the luminous flux decreases when we carry out of distance measurement that is close to maximum range. The relative fluctuations of luminous flux increase as well.

In our case, the intensity of the luminous flux decreases with the increasing of incidence angle on a diffusive surface in accordance with Lambert's law (Taylor 2000). Therefore, the error of phase registration as well as coefficient a increases when incidence angle increases to the limit value. The intensity decreasing of the reflected signal makes similar influence on relative error of the scale frequency $\frac{m_f}{f}$, which is included in the value of the coefficient b.

The next stage of an analytic model creating is the approximation of the parameters a and b, which are functions of the angle β. To select a type of functions for parameters a and b approximation we used the graphs constructed by the data from Table 3 (Fig. 5).

It is established that the change of coefficient a is best describedby a linear function, and coefficient b – by the exponential. The trend lines presented in Fig. 5 were created using Microsoft Excel. The value of coefficient of determination R^2 is 0.82 for linear approximation and 0.87 for exponential approximation. The regression models fit well.

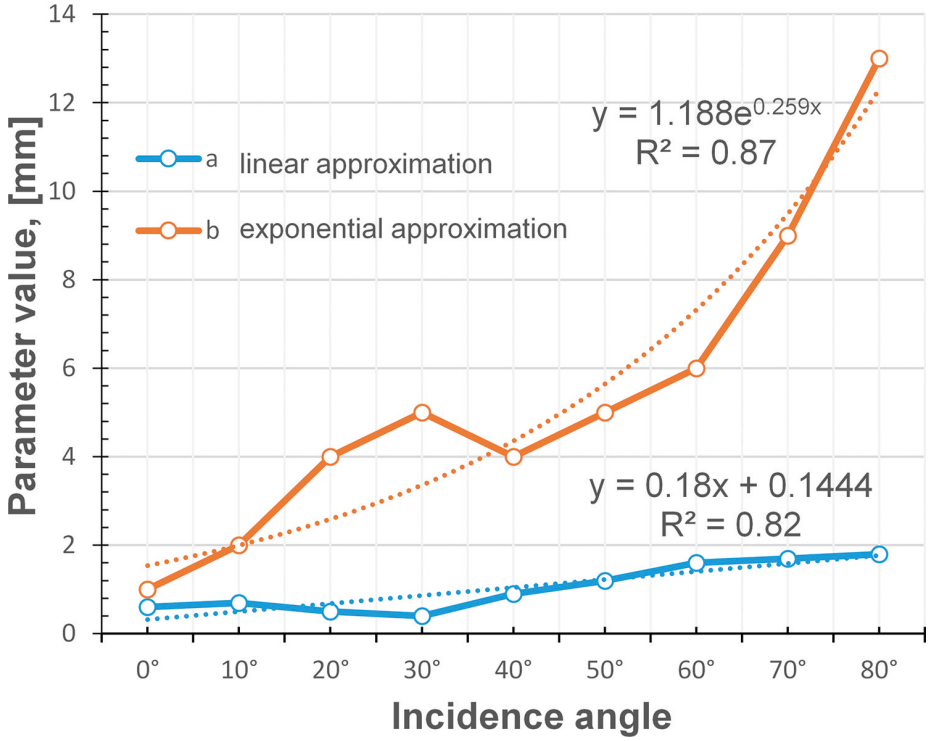

Fig. 5. *Trend approximation of obtained parameters a i b.*

According to data from Table 3 we write the linear regression equation for parameter a:

$$a = c \cdot \beta + d \,. \tag{31}$$

The coefficients $c$and d are determined by the least square method. Since the values of parameter a are obtained for different angles β, their values weights are unequal and are characterized by the weights p_i. The residual equations have the form:

$$c \cdot \beta + d - a_i = v_i \,, \tag{32}$$

and the weight matrix **P**, with the size 9×9, has the form:

$$\mathbf{P} = \begin{pmatrix} \frac{1}{\beta_1} & 0 & 0 & 0 \\ 0 & \frac{1}{\beta_2} & 0 & 0 \\ 0 & 0 & \ldots & 0 \\ 0 & 0 & 0 & \frac{1}{\beta_n} \end{pmatrix}. \tag{33}$$

After calculations were obtained the value of the parameter a:

$$a = 0.6\beta + 0.6\,, \tag{34}$$

where β expressed in radians.

Parameter b is approximated by the exponential regression equation with coefficients g and h:

$$b = g \cdot e^{h \cdot \beta}\,. \tag{35}$$

The coefficients have been found by the least square method with taking into account the weight matrix (Eq. 33).

For finding the log-linearized version of Eq. 35, logs were taken on both sides of the equation:

$$\ln b = \ln g + h \cdot \beta \cdot \ln e\,, \tag{36}$$

the variables rewrite using the identity $b' = \ln b$, $g' = \ln g$:

$$b' = h \cdot \beta + g'\,. \tag{37}$$

Then the residual equations have such form:

$$h \cdot \beta + g' - \ln b_i = v_i\,. \tag{38}$$

After performed calculations of coefficient g with taking into account the identity, we obtain the exponential regression equation of parameter b:

$$b = e^{2.1\beta}\,. \tag{39}$$

Rewrite Eq. 1, using obtained Eq. 34 and Eq. 39:

$$m_S = 0.6 + 0.6\beta + e^{2.1\beta} \cdot S \cdot 10^{-5}\ \text{mm}. \tag{40}$$

The accuracy equation (40) describes the cumulative influence of the distance and incidence angle on the distance measurement error in the reflectorless mode of the total station.

3. Discussion of the Results

Based on theoretical data (Schäfer 2017), obtained accyracy equation (40) consist of: coefficient 0.6 is the value of instrument constant (accuracy of coefficient determination $m = \pm 0.01$); 0.6β – a variable that shows total impact of the phase registration error and the error of voltage reference, which is proportional to the incidence angle (accuracy of coefficient determination $m = \pm 0.2$); $e^{2.1\beta}$ is a variable that takes into account the change in the relative error of the scale frequency (accuracy of coefficient determination $m = \pm 0.3$).

For evaluation of the goodness of accuracy equation (Eq. 40), a priory accuracy estimation of horizontal coordinates of the points on the pipeline was conducted. The distance measurement error m_s was calculated using Eq. 40.

In contrast to the widespread dependence $m_S = \pm(a + b \cdot S)$, the obtained formula takes into account not only the length of the measured distance but also the incidence angle to the observation surface. The error ellipses that presented in Fig. 6, show the relation between coordinate errors calculated by a priori and a posteriori accuracy estimation.

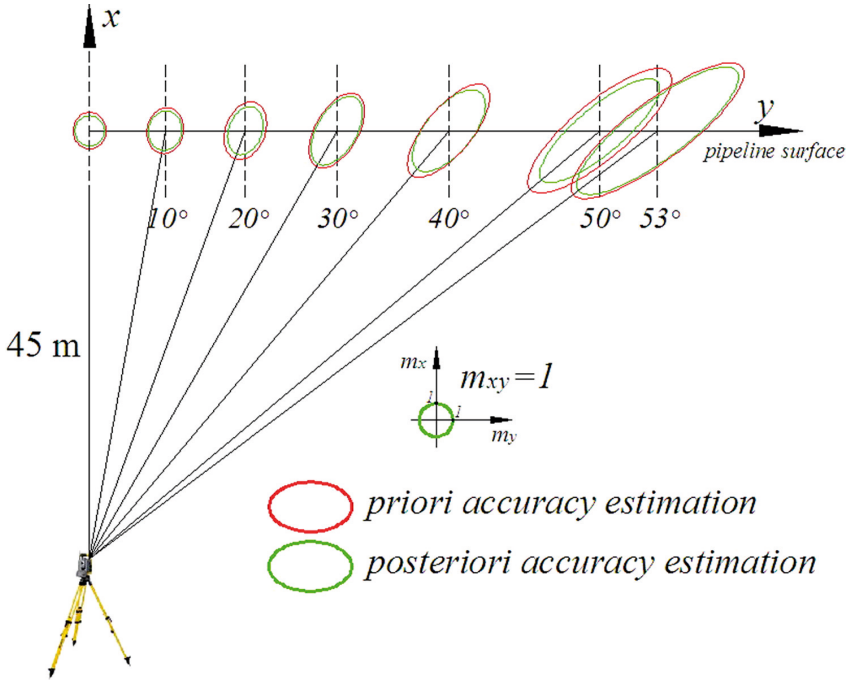

Fig. 6. *Error ellipses obtained by a priori and a posteriori accuracy estimation.*

In Fig. 6 we see that the size of error ellipses obtained by a priori accuracy estimation does not exceed error ellipses obtained from observation data. The application of Eq. 40 allows us to obtain a reliable value of coordinates error when performing a priori accuracy estimation.

4. Conclusions

The article presents an algorithm for a priori accuracy estimation of points coordinates on the above-ground pipeline's surface, which measured using a reflectorless total station. The results of a priori and a posteriori accuracy estimations of points coordinates were compared. It is established that for the beam's incidence

angles more than 37° the accuracy of the horizontal coordinates determining exceeds the theoretically calculated accuracy; the accuracy of the vertical coordinates determining exceeds the theoretically calculated values for the incidence angles of more than 33°.

The study results of the reflectorless mode of Sokkia 530RK total station for different distances and incidence angles to the pipeline surface are presented. The sources of distance measuring errors, using the total station in reflectorless mode, were analyzed. It was useful for the analytical representation of the obtained data.

The parameters of the accuracy equation of distance measurement were obtained using the least square method. The accuracy equation takes into account the distance and the laser beam's incident angle. The accuracy of the obtained parameters is determined. The obtained accuracy equation shows the relation between distance measurement error due to incidence angle and the length of a measured line. Its application allows obtaining a reliable value of the distance measurement error to perform a priori accuracy estimation.

References

Ali, S., Omar, N., Abujayyab, S. (2016): Investigation of the Accuracy of Surveying and Buildings with the Pulse (Non Prism) Total Station, International Journal of Advanced Research, 4 (3), 1518–1528.

Barković, Đ., Zrinjski, M., Baričević, S. (2016): Automation of Testing the Precision of Electro-Optical Distance Meters at the Calibration Baseline, Geodetski list, 70 (4), 311–336.

Daliga, K., Kuraĺowicz, Z. (2016): Examination Method of the Effect of the Incidence Angle of Laser Beam on Distance Measurement Accuracy to Surfaces with Different Colour and Roughness, Boletim de Ciências Geodésicas, 22 (3), 420–436.

Du, L., Zhong, R., Sun, H., Wu, Q. (2017): Automatic monitoring of tunnel deformation based on high density point clouds data, The International Archives of the Photogrammetry, Remote Sensing and Spatial Information Sciences, Volume XLII-2/W7.

Fan, H. (2010): Theory of Errors and Least Squares Adjustment, Royal Institute of Technology, Stockholm.

Fawzy, H. (2015): Evaluate the accuracy of reflector-less total station, International Journal of Civil Engineering and Technology, 6 (3), 23–30.

Gairns, C. (2008): Development of a Semi-automated System for Structural Deformation Monitoring Using a Reflectorless Total Station, M.Sc.E. thesis, Department of Geodesy and Geomatics Engineering Technical Report No. 255, University of New Brunswick, Fredericton, New Brunswick, Canada.

Jeźko, J. (2014): Calibration of surveying instruments and tools – means to the quality increase of deformation measurements, Journal of Sustainable Mining, 13 (4), 17–22.

Khalil, R. (2015): Accuracy Evaluation of Long-Range Reflectorless Distance Measurement, Positioning, 6, 61–70.

Kukhtar, D. (2017): Mathematical Modeling of Horizontal Displacement of Above-Ground Gas Pipelines, EUREKA: Physics and Engineering, 1 (8), 46–52.

Lambrou, E. (2018): Modeling the Deviations of the Reflectorless Distance Measurement Due to the Laser Beam's Incident Angle, International Journal of Applied Science and Technology, 8 (1), 11–23.

Lambrou, E., Pantazis, G. (2010): Evaluation of the Credibility of Reflectorless Distance Measurement, Journal of Surveying Engineering, 136 (4).

Lobachev, V. M. (1980): Radioelektronnaya geodeziya, Nedra, Moscow (in Russian).

Mazalová, J., Valentová, K., Vlćková, L. (2009): Testing of the accuracy of Leica TCRP 1201 total stations, Topcon GPT-7001 and Topcon GPT-8203M, Acta Montanistica Slovaca, Ročník, 14/1, 69–74.

Okwuashi, O., Asuquo, I. (2014): Basics of Least Squares Adjustment Computation in Surveying, International Journal of Science and Research, 3 (8), 188–193.

Rákay, Š., Zuzik, J., Weiss, G., Labant, S. (2013): Surveying of inaccessible rock faces and volume calculation of the irregular solids using robotic total station, Acta Montanistica Slovaca, Ročník, 18/3, 164–171.

Schäfer, T. (2017): Berührungslose und flächenhafte Deformationsmessungen an Betonoberflächen unter besonderer Berücksichtigung der Interaktion zwischen Laserstrahl und Oberfläche, Dissertation for: Dr.-Ing., Technischen Universität München, München.

Shults, R., Roshchyn, O. (2016): Preliminary Determination of Spatial Geodetic Monitoring Accuracy for Free Station Method, Geodetski list, 70 (4), 355–370.

Tamagnan, D., Beth, M. (2012): Remote monitoring of surface deformation with robotic total stations using reflectorless measurements (RRTS), Geotechnical News, 30.

Taylor, A. (2000): Illumination Fundamentals, Lighting Research Center.

Trevoho, I. S., Ilkiv, Ye. Yu., Kukhtar, D. V. (2011): Osoblyvosti vyznachennya prostorovoho polozhennya nadzemnykh perekhodiv mahistralnykh hazoprovodiv z vykorystannyam elektronnoho takheometra u bezreflektornomu rezhymi, Suchasni dosyahnennya heodezychnoyi nauky ta vyrobnytstva, 2 (22), 124–128 (in Ukrainian).

Zámećníková, M., Neuner, H., Pegritz, S. (2014): Influence of the Incidence Angle on the Reflectorless Distance Measurement in Close Range, INGEO 2014 – 6th International Conference on Engineering Surveying, Prague, Czech Republic, 257–262.

Modeliranje jednadžbe točnosti za geodetsku mjernu stanicu bez reflektora Sokkia 530RK s obzirom na upadni kut na površinu cjevovoda iznad zemlje

SAŽETAK. Specifičnost nadziranja cjevovoda iznad zemlje zahtijeva brza daljinska mjerenja. U većini je slučajeva nemoguće postaviti reflektirajuću prizmu na građevinske elemente radi mjerenja udaljenosti. Ovi se zahtjevi mogu ispuniti primjenom geodetske mjerne stanice kojom se mjeri bez reflektora. U radu su uspoređeni rezultati procjene točnosti a priori i a posteriori za određivanje koordinata cjevovoda pomoću geodetske mjerne stanice bez reflektora Sokkia 530RK. U ovom istraživanju provedena su laboratorijska i terenska ispitivanja te rezultati mjerenja na postojećem plinskom cjevovodu (promjer cijevi 1420 mm). Rezultati eksperimenata pokazali su da vrijednost pogreške horizontalnih koordinata prekoračuje očekivanu pogrešku za upadni kut veći od 37°. Vrijednosti pogrešaka vertikalnog položaja točaka prekoračuju teorijski izračunate vrijednosti za upadne kutove veće od 33°. Provedena je analiza izvora pogrešaka pri određivanju udaljenosti s geodetskom mjernom stanicom bez reflektora. Dobivena jednadžba točnosti na temelju eksperimentalnih podataka omogućava nam da odredimo pogrešku mjerenja udaljenosti ovisno o udaljenosti i upadnom kutu.

Ključne riječi: geodetska mjerna stanica bez reflektora, procjena točnosti a priori, upadni kut, nadziranje građevinskog objekta, cjevovod iznad zemlje.

Received / *Primljeno:* 2018-02-19

Accepted / *Prihvaćeno:* 2018-09-17